Electron-electron scattering in coupled quantum wells

M. Slutzky, O. Entin-Wohlman, Y. Berk, and A. Palevski
School of Physics and Astronomy, Raymond and Beverly Sackler Faculty of Exact Sciences, Tel Aviv University, Tel Aviv 69978, Israel

H. Shtrikman
Department of Condensed Matter, The Weizmann Institute of Science, Rehovot 76100, Israel
(Received 24 August 1995)

The inelastic electron-electron scattering rate in strongly coupled quantum wells is investigated. Both intrasubband and intersubband scattering processes are considered. The theoretical results are compared with experimental data obtained from the analysis of the resistance resonance measured on GaAs/Al_xGa_{1-x}As heterostructures in the presence of an in-plane magnetic field. A good agreement with the theoretical curves is obtained. The range of validity of the picture presented is discussed critically.

I. INTRODUCTION

The system of quantum wells (QW's) coupled by tunneling exhibits a number of interesting properties. For example, the resistance of two QW's with different mobilities connected in parallel strongly depends on the potential profile of the QW's and has a peak when the latter is symmetric.[1] This phenomenon is referred to as resistance resonance (RR) and has been studied to some extent during recent years.[2–4]

Recently, it has been demonstrated (both theoretically and experimentally[5]) that an in-plane magnetic field suppresses the RR. The magnitude of the effect depends on the coupling energy (Δ) between the wells and also on the width of the single-particle states ($\hbar/\tau$). Experimentally, it has been found that the main temperature dependence of $1/\tau$ is likely to emerge from electron-electron scattering. The comparison of the experimental values of $1/\tau^{ee}$ (as function of temperature) with the well–known theoretical expression for the inelastic rate in a two-dimensional electron gas[6] (2DEG) confirms this assumption.

This explanation is quite acceptable when the wells are weakly coupled. In that case, the electrons are not scattered between the wells and consequently the electron lifetime in one of the wells is not altered significantly by the presence of the second well. This picture, however, is not valid in the opposite limit of strongly coupled wells. When $\hbar/\Delta$ becomes smaller than any of the time scales in the problem, the stationary states of the electrons are extended over the two wells and the energy spectrum is modified accordingly. Therefore, the theoretical description of $1/\tau^{ee}$ has to be reviewed and compared with the relevant experimental results.

In this paper we present an extensive theoretical and experimental study of the inelastic electron-electron scattering rate in two strongly coupled QW's. The theory presented in Sec. II takes into account the two subbands that are formed in the system at resonance. We consider both intrasubband and intersubband scattering and derive asymptotic expressions appropriate for typical experimental situations. In Sec. III we present the experimental data of $1/\tau^{ee}$ obtained from the analysis of the resistance resonance measured on GaAs/Al_xGa_{1-x}As heterostructures in the presence of an in–plane magnetic field. The experimental values of $1/\tau^{ee}$ are compared with the theoretical curves. In the same section, we discuss critically the applicability of the present theory and indicate possible ways for its further verification. Section IV includes our conclusions.

II. THEORETICAL CALCULATIONS

A. Hamiltonian

Consider first the Schrödinger equation of our system disregarding the Coulomb interaction. We choose the z axis in the direction perpendicular to the plane of the QW's. Then the Hamiltonian splits into two parts: The first pertains to the free motion in the x-y plane and the second to the confined motion along the z axis. The latter produces a series of bound states. The eigenfunctions and the eigenvalues are therefore given by

$$\Psi_l(\mathbf{r}) = \exp(i\mathbf{kr})\,\phi_l(z), \tag{1}$$

$$\epsilon_l(\mathbf{k}) = E_l + \frac{\hbar^2 k^2}{2m^*}. \tag{2}$$

Here $\mathbf{r}$ is the two-dimensional (2D) coordinate in the x-y plane, $\mathbf{k}$ is the corresponding wave vector, m^* is the effective mass, and E_l is the discrete energy level that corresponds to the lth bound state. These relations define the *subband structure* of the spectrum. Due to the symmetry of the Hamiltonian, $\phi_l(z)$ has to be either of even ($l=1,3,5,\ldots$) or of odd ($l=2,4,6,\ldots$) parity.

In samples with the GaAs/Al_xGa_{1-x}As heterostructure, the barrier height is $\approx$300 meV. In our experiments, the width of each QW is 139 Å, and the thickness of the barrier (d) is typically 14–40 Å. At actual electronic densities ($\sim 5\times10^{11}$ cm^{-2}) only the two lowest subbands are populated (Fig. 1). The separation (Δ) between the two lowest subbands vanishes exponentially as d is increased. For the range of barrier thicknesses mentioned above, Δ is typically $\sim 2.2-0.6$ meV. The Fermi energy ϵ_F is $\sim$10 meV. The z wave function corresponding to the lower subband ($l=1$) is symmetric, and that of the next subband ($l=2$) is antisymmetric. These properties will be used in the calculation of the matrix elements of the Coulomb interactions.

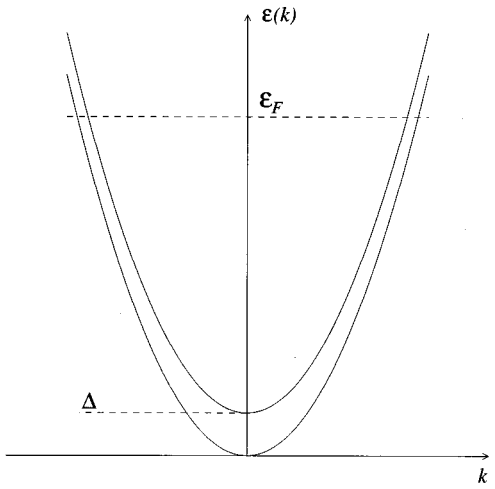

FIG. 1. The energy spectrum of the coupled quantum wells.

The general Coulomb interaction in our two subband system can be written in the form

$$H_c=\frac{1}{2}V_{l_1l_2l_3l_4}(\mathbf{q})c^{\dagger}_{l_1\mathbf{k}+\mathbf{q}\sigma_1}c^{\dagger}_{l_2\mathbf{p}-\mathbf{q}\sigma_2}c_{l_4\mathbf{p}\sigma_2}c_{l_3\mathbf{k}\sigma_1},\quad l_i=1,2, \tag{3}$$

where $c^{\dagger}_{l\mathbf{k}\sigma}$ ($c_{l\mathbf{k}\sigma}$) is the creation (annihilation) operator for an electron in the lth subband having wave vector $\mathbf{k}$ and spin projection σ,

$$V_{l_1l_2l_3l_4}(\mathbf{q})=\frac{2\pi e^2}{q\varepsilon}\int dz_1dz_2\phi_{l_1}(z_1)\phi_{l_2}(z_1)\phi_{l_3}(z_2)\phi_{l_4}(z_2)\times\exp[-q|z_1-z_2|], \tag{4}$$

in which ε is the dielectric constant of the background medium (GaAs) and the repeated indices are summed over. In the following we shall discard the exchange Coulomb interactions, as their effect is likely to be small.

Since the parity of the two particle wave function has to be conserved, the only nonvanishing matrix elements are

$$V_{1111}=V_1,\quad V_{2222}=V_2,\quad V_{1212}=V_{2121}=V_3,$$
$$V_{1122}=V_{2211}=V_4,\quad V_{1221}=V_{2112}=V_5. \tag{5}$$

The elements V_1, V_2, and V_3 are the amplitudes for the processes in which the electrons remain in their respective subbands (*intrasubband* interactions), whereas the elements V_4 and V_5 correspond to the *intersubband* interaction, i.e., processes transferring each of the interacting electrons to the other subband. The functions $\phi_l(z)$ are real, and therefore $V_4=V_5$.

The Coulomb interactions that give rise to the inelastic decay rate of the electrons are screened. We present in the Appendix the derivation of the dynamically screened Coulomb interaction, $\Gamma_{ll_1l_2l_3}(\mathbf{q},\omega)$, within the random-phase approximation. We also show there that it is sufficient to use the static limit for the screening in the calculation of the relaxation rate.[7–9]

B. Calculation of the rate

As we consider only two subbands, we adopt the two-band formalism for the calculation of the scattering rate resulting from the Coulomb interactions. The inelastic rate for an electron in the lth subband, averaged over the Fermi surface, has the form[7]

$$\frac{1}{\tau_l^{ee}}=\frac{2\pi\beta}{N_0\hbar}\sum_{l_1,l_2,l_3}\sum_{\mathbf{k},\mathbf{p},\mathbf{q},\sigma,\sigma'}|\Gamma_{ll_1l_2l_3}(\mathbf{q})|^2\delta[\epsilon_{l_2}(\mathbf{k}+\mathbf{q})+\epsilon_{l_3}(\mathbf{p}-\mathbf{q})-\epsilon_l(\mathbf{k})-\epsilon_{l_1}(\mathbf{p})]\times f^0_{l,\sigma}(\mathbf{k})f^0_{l_1,\sigma'}(\mathbf{p})[1-f^0_{l_2,\sigma}(\mathbf{k}+\mathbf{q})][1-f^0_{l_3,\sigma'}(\mathbf{p}-\mathbf{q})], \tag{6}$$

where $\beta=1/k_BT$, N_0 is the 2D density of states and

$$f^0_{l,\sigma}(\mathbf{k})=f^0_l(\mathbf{k})=\frac{1}{\exp[\beta(\epsilon_l(\mathbf{k})-\epsilon_F)]+1} \tag{7}$$

is the equilibrium Fermi distribution function.

The expression for $1/\tau_l^{ee}$ can be put in a form that is more convenient for the calculation. Introducing the generalized (for the two-band case) polarization

$$\Pi_{ll'}(\mathbf{q},\omega)=\sum_{\mathbf{k},\sigma}\frac{f^0_{l,\sigma}(\mathbf{k}-\mathbf{q})-f^0_{l',\sigma}(\mathbf{k})}{\hbar\omega+i\eta+\epsilon_l(\mathbf{k}-\mathbf{q})-\epsilon_{l'}(\mathbf{k})}, \tag{8}$$

and noting that

$$\sum_{\mathbf{k},\sigma}f^0_{l,\sigma}(\mathbf{k})[1-f^0_{l',\sigma}(\mathbf{k}+\mathbf{q})]\delta[\epsilon_{l'}(\mathbf{k}+\mathbf{q})-\epsilon_l(\mathbf{k})-\hbar\omega]=\frac{1}{\pi(e^{-\beta\hbar\omega}-1)}\mathrm{Im}[\Pi_{ll'}(\mathbf{q},\omega)] \tag{9}$$

we finally obtain

$$\frac{1}{\tau_l^{ee}} = -\frac{\beta}{2\pi N_0} \sum_{l_1,l_2,l_3} \int_{-\infty}^{\infty} \frac{d\omega}{\sinh^2(\beta\hbar\omega/2)} \sum_{\mathbf{q}} |\Gamma_{ll_1l_2l_3}(\mathbf{q})|^2 \chi_{ll_2}(\mathbf{q},\omega)\chi_{l_1l_3}(\mathbf{q},-\omega), \tag{10}$$

where the susceptibility $\chi_{ll_2}(\mathbf{q},\omega)$ is the imaginary part of the generalized polarization. This quantity is calculated in the Appendix.

Next we consider the possible channels for scattering. The total scattering rate can be separated into the rate resulting from the intersubband transitions and that coming from the intrasubband processes,

$$\left(\frac{1}{\tau_l^{ee}}\right)^{\text{tot}} = \left(\frac{1}{\tau_l^{ee}}\right)^{\text{inter}} + \left(\frac{1}{\tau_l^{ee}}\right)^{\text{intra}}. \tag{11}$$

For instance, for $1/\tau_1^{ee}$ we write

$$\left(\frac{1}{\tau_1^{ee}}\right)^{\text{intra}} = -\frac{\beta}{2\pi N_0} \int_{-\infty}^{\infty} \frac{d\omega}{\sinh^2(\beta\hbar\omega/2)} \sum_{\mathbf{q}} \{|\Gamma_{1111}(\mathbf{q})|^2 \chi_{11}(\mathbf{q},\omega)\chi_{11}(\mathbf{q},-\omega) + |\Gamma_{1212}(\mathbf{q})|^2 \chi_{11}(\mathbf{q},\omega)\chi_{22}(\mathbf{q},-\omega)\}, \tag{12}$$

$$\left(\frac{1}{\tau_1^{ee}}\right)^{\text{inter}} = -\frac{\beta}{2\pi N_0} \int_{-\infty}^{\infty} \frac{d\omega}{\sinh^2(\beta\hbar\omega/2)} \sum_{\mathbf{q}} |\Gamma_{1122}(\mathbf{q})|^2 \{\chi_{12}(\mathbf{q},\omega)\chi_{12}(\mathbf{q},-\omega) + \chi_{12}(\mathbf{q},\omega)\chi_{21}(\mathbf{q},-\omega)\}. \tag{13}$$

Similar expressions hold for $1/\tau_2^{ee}$.

In order that the integral over ω will converge, the numerator of the integrand should vanish at $\omega\to 0$ at least as $O(\omega^{1+\delta})$. For the intrasubband susceptibilities $\chi_{ii}(\mathbf{q},-\omega) = -\chi_{ii}(\mathbf{q},\omega)$, and therefore the product $\chi_{ii}(\mathbf{q},\omega)\chi_{ll}(\mathbf{q},-\omega)$ is necessarily even in ω, leading to the desired convergence. The situation is more delicate for the intersubband part of the total rate. In this case

$$\chi_{12}(\mathbf{q},-\omega) = -\chi_{21}(\mathbf{q},\omega), \quad \chi_{12}(\mathbf{q},0) \neq 0. \tag{14}$$

Using this property, we can write the ω integration in Eq. (13) in a symmetrized form

$$\int_{-\infty}^{\infty} d\omega \sum_{\mathbf{q}} \frac{\chi_{12}(\mathbf{q},\omega)\chi_{21}(\mathbf{q},-\omega)}{\sinh^2(\beta\hbar\omega/2)} + \int_{-\infty}^{\infty} d\omega \sum_{\mathbf{q}} \frac{\chi_{12}(\mathbf{q},\omega)\chi_{12}(\mathbf{q},-\omega)}{\sinh^2(\beta\hbar\omega/2)} = -\frac{1}{2}\int_{-\infty}^{\infty} d\omega \sum_{\mathbf{q}} \frac{[\chi_{12}(\mathbf{q},-\omega) - \chi_{12}(\mathbf{q},\omega)]^2}{\sinh^2(\beta\hbar\omega/2)}. \tag{15}$$

This integral has no singularities at $\omega\to 0$.

For the sake of comparison with the experimental data, the rates $1/\tau_{1,2}^{ee}$ have been evaluated numerically for various values of Δ and ϵ_F for temperatures ranging from 1 to 40 K (see the discussion in the next section). However, one can also derive asymptotic formulas for the intrasubband and intersubband scattering rates as functions of ϵ_F, Δ, and T for the actual experimental situations.

Under the experimental conditions, one usually has

$$\epsilon_F \gg \Delta, k_B T. \tag{16}$$

For the lowest temperatures considered (1–10 K), $\Delta \gg k_B T$. At elevated temperatures, Δ and $k_B T$ become of the same order so that at 30–40 K we may have $\Delta \leqslant k_B T$. As we shall see, the intersubband rate is strongly affected by the relative magnitudes of Δ and $k_B T$ whereas the intrasubband rate is almost independent of it as long as (16) holds. This is quite expected, since the intrasubband rate involves the intrasubband susceptibilities χ_{11} and χ_{22}, which are to a good approximation Δ independent.

For the purposes of estimate we may put for the screened Coulomb matrix elements

$$\Gamma_{ll_1l_2l_3} \sim 1/2N_0. \tag{17}$$

Then the first sum over $\mathbf{q}$ in (12), to lowest order in ω, gives

$$\sum_{\mathbf{q}} \chi_{11}(\mathbf{q},\omega)\chi_{11}(\mathbf{q},-\omega) \sim N_0^2 k_F^2 \left\{ \alpha_1 \left(\frac{\hbar\omega}{\epsilon_F}\right)^2 - \alpha_2 \left(\frac{\hbar\omega}{\epsilon_F}\right)^2 \ln\left(\frac{4\epsilon_F}{|\hbar\omega|}\right)\right\}, \tag{18}$$

where k_F is the Fermi vector of the lowest subband and α_i are positive numerical constants of order unity. Since $\epsilon_F \gg \Delta$, it is clear that

$$\sum_{\mathbf{q}} \chi_{11}(\mathbf{q},\omega)\chi_{22}(\mathbf{q},-\omega) \approx \sum_{\mathbf{q}} \chi_{11}(\mathbf{q},\omega)\chi_{11}(\mathbf{q},-\omega). \tag{19}$$

Integrating over ω we obtain

$$\left(\frac{\hbar}{\tau_1^{ee}}\right)^{\text{intra}} \sim -A_1\frac{(k_BT)^2}{\epsilon_F} + A_2\frac{(k_BT)^2}{\epsilon_F}\ln\left(\frac{4\epsilon_F}{k_BT}\right), \tag{20}$$

where A_i are positive numerical constants of order unity. This form for the relaxation rate in the intrasubband channel is not unexpected. Due to the presence of the second subband, the phase space for the intrasubband rate is roughly twice that of the single-band one (i.e., the usual rate in the case of 2DEG). Also, the screening of the interaction is roughly twice more effective (see the Appendix; note that this factor is doubled in the expression for the relaxation rate). Thus, the resulting expression should be equal to the expression for 2DEG within a factor of order unity.

Next we consider the intersubband rate in the limit $\Delta > k_BT$. Using Eq. (15), the $\mathbf{q}$ integration to lowest order in ω yields

$$\sum_{\mathbf{q}} [\chi_{12}(\mathbf{q},\omega)-\chi_{12}(\mathbf{q},-\omega)]^2 \sim N_0^2k_F^2\left\{-\gamma_1\left(\frac{\hbar\omega}{\epsilon_F}\right)^2 + \gamma_2\left(\frac{\hbar\omega}{\epsilon_F}\right)^2\ln\left(\frac{4\epsilon_F}{\Delta}\right) + \gamma_3\left(\frac{\hbar\omega}{\epsilon_F}\right)^2\ln\left(\frac{\Delta}{|\hbar\omega|}\right)\right\}, \tag{21}$$

where γ_i are positive numerical constants with $\gamma_2 \gg \gamma_3$. Integrating over the frequency, we find

$$\left(\frac{\hbar}{\tau_1^{ee}}\right)^{\text{inter}} \sim -B_1\frac{(k_BT)^2}{\epsilon_F} + B_2\frac{(k_BT)^2}{\epsilon_F}\ln\left(\frac{4\epsilon_F}{\Delta}\right) + B_3\frac{(k_BT)^2}{\epsilon_F}\ln\left(\frac{\Delta}{k_BT}\right). \tag{22}$$

Here B_i are positive numerical constants with $B_2 \gg B_3$. It is not difficult to understand the physical meaning of this expression. When $\Delta \gg k_BT$, the average energy transfer in an inelastic collision event is small compared to Δ. Energy conservation then imposes a restriction on the available phase space. The cutoff of the momentum transfer is now $\sim(\Delta/2\epsilon_F)k_F$ [instead of the value $\sim(k_BT/2\epsilon_F)k_F$ in the intrasubband case] so that Δ replaces k_BT in the logarithm. The term containing $\ln(\Delta/k_BT)$ is a correction to the latter. At higher temperatures (when $\Delta < k_BT$), the average energy transfer is larger than Δ. Then the cutoff value of the momentum transfer is again $\sim(\hbar\omega/2\epsilon_F)k_F$ and

$$\chi_{12}(\mathbf{q},\omega) \sim \chi_{11}(\mathbf{q},\omega). \tag{23}$$

Therefore, in this limit Eq. (13) would yield the expression (20) for the intrasubband rate.

III. EXPERIMENT

Two sets of double QW structures were grown on a semi-insulating GaAs substrate by molecular-beam epitaxy. They consist of two GaAs wells of 139-Å width separated by 14-Å and 28-Å $Al_{0.3}Ga_{0.7}As$ barriers. The electrons were provided by remote δ-doped donor layers set back from the top and the bottom wells by spacer layers. In all our samples the bottom well had lower mobility due to the rougher $GaAs/Al_xGa_{1-x}As$ interface for that well.

Measurements were done on 10-μm-wide and 200-μm-long channels with Au/Ge/Ni Ohmic contacts. Top and bottom gates were patterned using the standard photolithography fabrication method. The top Schottky gate covered 150 μm of the channel. The data were taken using a lock-in four-terminal technique at $f = 37$ Hz. The voltage probes connected to the gated segment of the channel were separated by 100 μm.

The variation of the top gate voltage, V_g, allows one to sweep the potential profile of the QW's through the resonance configuration. The resistance versus the top gate voltage for the sample with a 28-Å barrier at $T = 4.2$ K is plotted in the inset of Fig. 2. The resistance resonance is clearly observed at $V_g \approx 0.28$ V. A similar procedure allows one to determine the resonance values of V_g for the structures with a 14-Å barrier. We next fix the gate voltages at the values corresponding to the exact resonance positions, and measure the resistance as a function of the in-plane magnetic field perpendicular to the direction of the current, $\mathbf{H} \perp \mathbf{j}$. Figure 2 shows the behavior of the RR for the two structures with 14-Å and 28-Å barriers.

The experimental data clearly demonstrate the suppression of the RR by the magnetic field, as well as the expected broadening for the more strongly coupled structures: The resistance decreases more slowly for the samples with the smaller barrier width. According to Ref. 5, the dependence of the resonance resistance on H is given by

$$R^{-1}(H) - R_{\text{off}}^{-1} = [R^{-1}(0) - R_{\text{off}}^{-1}]f(H/H_c), \tag{24}$$

$$f(x) = \frac{2(\sqrt{1+x^2}-1)}{x^2\sqrt{1+x^2}}, \tag{25}$$

in which the characteristic field H_c is given by

$$H_c = \frac{\hbar c}{e}\frac{1}{v_F\tau b}\sqrt{1+\left(\frac{\Delta}{\hbar}\right)^2\frac{\tau_1^{\text{tr}}+\tau_2^{\text{tr}}}{2}\tau}. \tag{26}$$

Here $\tau_{1,2}^{\text{tr}}$ are the transport scattering times in the first and the second QW, respectively, v_F is the Fermi velocity, and b is the distance between the centers of the QW's. In the calculation,[5] $1/\tau$ results from the imaginary part of the self-energy correction. $R(0)$ and R_{off} are the values of the resistance at $H = 0$ and at saturation (at $H \gg H_c$), respectively.

The theoretical expression (24) fits perfectly the experimental data shown in Fig. 3 with τ being the *only* fitting

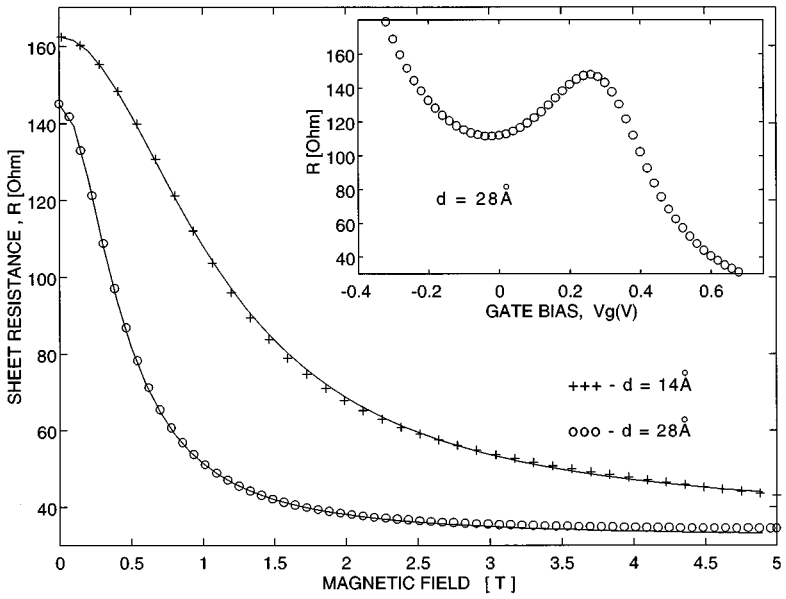

FIG. 2. The resonance resistance (RR) vs magnetic field at 4.2 K. The solid lines are computed from Eq. (24). The inset shows the line shape of the RR vs the top gate voltage.

parameter (see below). This fitting is carried out for several values of the temperature, and hence allows the determination of τ as function of T. As the temperature is increased, the experimental curves become broader and therefore $\tau(T)$ attains smaller values. The values of the scattering rate $1/\tau$ are temperature independent (within the experimental resolution) below 4.2 K for low-mobility samples and below 2.2 K for high-mobility samples. Hence it is plausible to assume that

$$\frac{1}{\tau(T)}=\frac{1}{\tau(0)}+\frac{1}{\tau^{ee}(T)}, \tag{27}$$

where $1/\tau(0)$ is the small-angle scattering rate that arises from elastic scattering processes and is therefore assumed to be temperature independent. The saturation values of the rate $[1/\tau(0)]$ are subtracted from $1/\tau(T)$ and the variation of $1/\tau(T)-1/\tau(0)$ is plotted versus temperature for samples with different barrier thicknesses (Fig. 4).

In order to deduce the microscopic parameters employed in the theoretical description we perform an analysis of Shubnikov–de Haas (SdH) oscillations of the resistance, for the samples with applied gate voltage corresponding to the RR. Fig. 3 shows beats of the resistance, which are an indication of the existence of two subbands with different Fermi wave vectors that are present at resonance.[10] The measurements of the SdH oscillations were performed at $T=0.28$ K. The distance between the nodes of the curve allows us to find the separation Δ between the subbands. For the samples with 14- and 28-Å barriers we obtain for Δ the values 2.3 and 1.1 meV, respectively. The complementary measurements of the Hall effect and the sample resistance versus gate voltage provide us with the rest of the parameters required for the definition of H_c, namely, $\tau_{1,2}^{\mathrm{tr}}$.

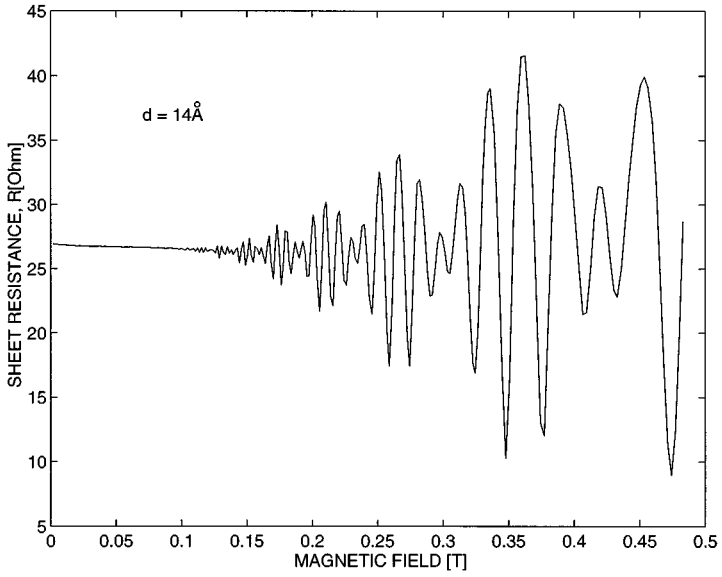

FIG. 3. Shubnikov–de Haas oscillations for the sample with barrier thickness $d=14$ Å.

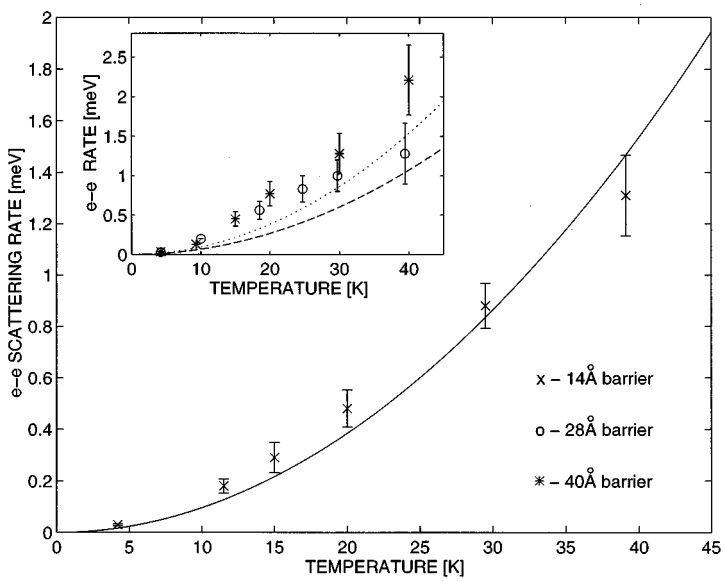

FIG. 4. The electron-electron scattering rate vs temperature. The solid line is computed from Eq. (10) for $\Delta = 2.3$ meV, $\epsilon_F = 7.6$ meV (barrier thickness, 14 Å). The dotted line corresponds to $\Delta = 1.1$ meV, $\epsilon_F = 7.5$ meV (barrier thickness, 28 Å), the dashed line to $\Delta = 0.6$ meV, $\epsilon_F = 10.9$ meV (barrier thickness, 40 Å).

In Fig. 4 we also present the curves of the inelastic scattering rate $1/\tau_1^{ee}$ for the actual values of ϵ_F and Δ, calculated from Eq. (10). It is clear that as long as $\epsilon_F \gg \Delta$, the two rates $1/\tau_{1,2}^{ee}$ are almost equal. Numerical calculations show that for the values of ϵ_F and Δ under consideration, this equality holds within few percent.

The agreement between the experimental points and the theoretical curves is quite remarkable for the sample with the 14-Å barrier. For the samples with 28- and 40-Å barriers, the deviations of the experimental values from the theoretical ones are relatively large (the data for the 40-Å barrier sample is taken from Ref. 5). This is not surprising since the two-band model is applicable only when $\hbar/\Delta$ is the shortest time scale in the problem. Otherwise, the bands are not well defined and a good agreement is not expected. For instance, even for the extremely clean samples, for which the main level broadening would have come from the interaction between the electrons, the two-band picture is not adequate for

$$\frac{1}{\tau(T)} \simeq \frac{1}{\tau^{ee}} \sim \frac{\Delta}{\hbar} . \tag{28}$$

For example, for the 14-Å barrier thickness ($\Delta = 2.3$ meV) this happens at $T \sim 60$ K. For more weakly coupled structures for which $\Delta \simeq 0.5-1$ meV, the range of validity of the present theory, using the criterion (28), is

$$T \leqslant 25-40 \text{ K}. \tag{29}$$

When impurities are present, this range is further decreased. For instance, in the samples with 14-, 28-, and 40-Å barriers, $1/\tau(0)$ was found to be 0.6, 0.84, and 1.85 meV, respectively. Thus, the sample with the 14-Å barrier is expected to follow the present theory up to $T \approx 40$ K. In the sample with the 28-Å barrier thickness, the two bands are poorly defined above $T \approx 15$ K. The 40-Å barrier sample clearly *cannot* be described by the present theory. Another well-known effect of the impurities is to increase the electron-electron scattering rate.[11] This increase results from the loss of momentum conservation, which in turn leads to a larger available phase space.

In order to verify other aspects of our calculation, e.g., the dependence of $1/\tau^{ee}$ on Δ and ϵ_F, it is insufficient to use only the heterostructures discussed here. It is possible (see Ref. 5) to produce samples with variable ϵ_F—this option is included by fabricating samples with two (top and bottom) gates. Unfortunately, the only way to study the Δ dependence of the rate is to grow samples with various values of barrier thickness.

Finally, we note that, strictly speaking, the calculation that yields expression (24) takes into consideration only elastic scattering processes. The perfect agreement of the experimental data with (24) at elevated temperatures, where inelastic processes are important, suggests that the latter can be incorporated by writing $1/\tau(T)$ in the form (27). However, a rigorous calculation of the resonant magnetoresistance that would take into account the electron-electron interaction has not yet been performed.

IV. CONCLUSIONS

We have calculated the electron-electron scattering rate in a system of two coupled QW's in second-order perturbation theory. We find that there exist two main contributions to the total rate: The intrasubband and the intersubband rates. It is shown that the intrasubband and intersubband interactions are screened with different dielectric functions that depend on the distance between the centers of the wells. The intrasubband rate exhibits the well-known $T^2 \ln T$ temperature dependence whereas the leading term in the expression for the intersubband rate is of the form $T^2 \ln \Delta$. This is due to the different values of the momentum transfer cutoff in the two scattering channels.

We have performed resonant magnetoresistance measurements on a set of $GaAs/Al_xGa_{1-x}As$ heterostructures with various values of barrier thickness. The temperature-dependent part of $1/\tau$ scales with temperature as T^2 and exhibits a good agreement with the theoretically calculated curve for the strongly coupled structure ($d = 14$ Å, $\Delta = 2.3$ meV). For more weakly coupled wells ($d = 40$ Å, $\Delta = 0.55$ meV and $d = 28$ Å, $\Delta = 1.1$ meV), the deviations of the ex-

perimental values of $1/\tau^{ee}$ from the corresponding theoretical ones are relatively large. This is attributed mainly to elastic scattering. The latter reduces the range of validity of our basic assumptions. Elastic scattering also increases the electron-electron scattering rate by relaxing the momentum conservation condition. This may partially explain the systematic positive deviations of the measured values of $1/\tau^{ee}$ from the theoretical curves.

ACKNOWLEDGMENTS

We thank A. Kamenev for helpful discussions. This research was supported in part by the Israel Academy of Sciences and Humanities, the U.S.-Israel Binational Science Foundation, and the German-Israel Foundation for Scientific Research and Development. Y.B. is supported by the Wejc Foundation.

APPENDIX: SCREENING OF THE COULOMB INTERACTIONS

Here we obtain the screened matrix elements of the Coulomb interactions within the random-phase approximation. Disregarding the exchange effects, the dynamically screened matrix elements $\Gamma_{l_1l_2l_3l_4}(\mathbf{q},\omega)$ are given by the Dyson equation

$$\Gamma_{l_1l_2l_3l_4}(\mathbf{q},\omega)=V_{l_1l_2l_3l_4}(\mathbf{q})+\sum_{mn} V_{l_1nl_3m}(\mathbf{q})\Pi_{nm}(\mathbf{q},\omega)\Gamma_{ml_2nl_4}(\mathbf{q},\omega), \tag{A1}$$

where $\Pi_{nm}(\mathbf{q},\omega)$ is the generalized polarization part given by (8). Inserting in (A1) the bare Coulomb matrix elements (5), one finds that the screened intrasubband elements, $\Gamma_{1111}=\Gamma_1,\Gamma_{2222}=\Gamma_2,\Gamma_{1212}=\Gamma_{2121}=\Gamma_3$ are given in terms of V_1,V_2, and V_3 alone,

$$\Gamma_1(\mathbf{q},\omega)=\frac{V_1(\mathbf{q})+\Pi_{22}(\mathbf{q},\omega)[V_3^2(\mathbf{q})-V_1(\mathbf{q})V_2(\mathbf{q})]}{D_1(\mathbf{q},\omega)}, \tag{A2}$$

$$\Gamma_2(\mathbf{q},\omega)=\frac{V_2(\mathbf{q})+\Pi_{11}(\mathbf{q},\omega)[V_3^2(\mathbf{q})-V_1(\mathbf{q})V_2(\mathbf{q})]}{D_1(\mathbf{q},\omega)}, \tag{A3}$$

$$\Gamma_3(\mathbf{q},\omega)=\frac{V_3(\mathbf{q})}{D_1(\mathbf{q},\omega)}, \tag{A4}$$

where

$$D_1(\mathbf{q},\omega)=[1-\Pi_{11}(\mathbf{q},\omega)V_1(\mathbf{q})][1-\Pi_{22}(\mathbf{q},\omega)V_2(\mathbf{q})]-\Pi_{11}(\mathbf{q},\omega)\Pi_{22}(\mathbf{q},\omega)V_3^2(\mathbf{q}). \tag{A5}$$

These involve the intrasubband polarizations Π_{11} and Π_{22}. Similarly, the screened intersubband elements Γ_{1122} and Γ_{1221} are given by V_4 and V_5, and the intersubband polarizations Π_{12} and Π_{21},

$$\Gamma_{1122}(\mathbf{q},\omega)=\frac{V_4(\mathbf{q})}{D_2(\mathbf{q},\omega)}, \tag{A6}$$

$$\Gamma_{1221}(\mathbf{q},\omega)=\frac{V_5(\mathbf{q})-\Pi_{12}(\mathbf{q},\omega)[V_4^2(\mathbf{q})-V_5^2(\mathbf{q})]}{D_2(\mathbf{q},\omega)}, \tag{A7}$$

with

$$D_2(\mathbf{q},\omega)=[1-\Pi_{12}(\mathbf{q},\omega)V_5(\mathbf{q})][1-\Pi_{21}(\mathbf{q},\omega)V_5(\mathbf{q})]-\Pi_{12}(\mathbf{q},\omega)\Pi_{21}(\mathbf{q},\omega)V_4^2(\mathbf{q}). \tag{A8}$$

Since in our case $V_4=V_5$, it follows that $\Gamma_{1122}=\Gamma_{1221}\equiv\Gamma_4$.

The evaluation of the screened matrix elements necessitates the calculation of the polarization parts. We find (at zero temperature)

$$\begin{aligned}\mathrm{Re}[\Pi_{ll'}(\mathbf{q},\omega)]&=\frac{2}{(2\pi)^2}\int d^2\mathbf{k}\ \frac{f_l(\mathbf{k}-\mathbf{q})-f_{l'}(\mathbf{k})}{\hbar\omega+\epsilon_l(\mathbf{k}-\mathbf{q})-\epsilon_{l'}(\mathbf{k})}\\&=-N_0\Bigg\{1-\frac{\mathrm{sgn}(q/2-\nu_{ll'}/2q)}{q}\Theta\left(\frac{|\nu_{ll'}-q^2|}{2qk_{Fl}}-1\right)\sqrt{\left(\frac{\nu_{ll'}-q^2}{2q}\right)^2-k_{Fl}^2}\\&\quad-\frac{\mathrm{sgn}(q/2+\nu_{ll'}/2q)}{q}\Theta\left(\frac{|\nu_{ll'}+q^2|}{2qk_{Fl'}}-1\right)\sqrt{\left(\frac{\nu_{ll'}+q^2}{2q}\right)^2-k_{Fl'}^2}\Bigg\},\end{aligned} \tag{A9}$$

where

$$\nu_{ll'}=2m^*(\hbar\omega+E_l-E_{l'})/\hbar^2. \tag{A10}$$

We have used here the dispersion relation (2). The Fermi wave vector of the lth subband is denoted k_{Fl}. The imaginary part of the polarizabiliy $\mathrm{Im}[\Pi_{ll'}(\mathbf{q},\omega)]=\chi_{ll'}(\mathbf{q},\omega)$ is given by

$$\begin{aligned}\chi_{ll'}(\mathbf{q},\omega)&=-\frac{2\pi}{(2\pi)^2}\int d^2\mathbf{k}[f_l(\mathbf{k}-\mathbf{q})-f_{l'}(\mathbf{k})]\delta[\hbar\omega+\epsilon_l(\mathbf{k}-\mathbf{q})-\epsilon_{l'}(\mathbf{k})]\\&=-\frac{N_0}{q}\Bigg(\Theta\left(1-\left|\frac{\nu_{ll'}}{2qk_{Fl}}-\frac{q}{2k_{Fl}}\right|\right)\left\{k_{Fl}^2-\left[\frac{\nu_{ll'}}{2q}-\frac{q}{2}\right]^2\right\}^{1/2}\\&\quad-\Theta\left(1-\left|\frac{\nu_{ll'}}{2qk_{Fl'}}+\frac{q}{2k_{Fl'}}\right|\right)\left\{k_{Fl'}^2-\left[\frac{\nu_{ll'}}{2q}+\frac{q}{2}\right]^2\right\}^{1/2}\Bigg).\end{aligned} \tag{A11}$$

The bare Coulomb matrix elements (5) can be safely approximated by

$$V_{1,2,3}(q) \simeq \frac{\pi e^2}{q\varepsilon}(1+\exp[-bq]),$$

$$V_{4,5}(q) \simeq \frac{\pi e^2}{q\varepsilon}(1-\exp[-bq]), \tag{A12}$$

where b is the distance between the centers of the QW's. This yields that the intrasubband elements are screened with the dielectric function

$$D_1(\mathbf{q},\omega) \simeq 1-\frac{\pi e^2}{q\varepsilon}[\Pi_{11}(\mathbf{q},\omega)+\Pi_{22}(\mathbf{q},\omega)] \times(1+\exp[-bq]), \tag{A13}$$

whereas the intersubband elements are screened with the dielectric function

$$D_2(\mathbf{q},\omega) = 1-\frac{\pi e^2}{q\varepsilon}[\Pi_{12}(\mathbf{q},\omega)+\Pi_{21}(\mathbf{q},\omega)] \times(1-\exp[-bq]). \tag{A14}$$

Here we exploit the fact that $V_4 = V_5$.

Using the results obtained above for the real and imaginary parts of the polarization, we find that the dielectric functions can be approximated by their *static* limits

$$D_1(\mathbf{q}) \simeq 1+\frac{2\pi e^2 N_0}{q\varepsilon}(1+\exp[-bq]), \tag{A15}$$

$$D_2(\mathbf{q}) \simeq 1+\frac{2\pi e^2 N_0}{q\varepsilon}(1-\exp[-bq]), \tag{A16}$$

with small imaginary corrections of order $k_F\hbar\omega/2q\epsilon_F$, which appear only for $q > m^*\omega/\hbar k_F$. In these estimates it is sufficient to assume $k_{F1} \sim k_{F2} \sim k_F$.

[1] A. Palevski, F. Beltram, F. Capasso, L. N. Pfeiffer, and K. W. West, Phys. Rev. Lett. **65**, 1929 (1990).

[2] A. Palevski, S. Luryi, P. L. Gammel, F. Capasso, L. N. Pfeiffer and K. W. West, Superlatt. Microstruct. **11**, 269 (1992).

[3] Y. Ohno, M. Tsuchia, and H. Sakaki, Appl. Phys. Lett. **62**, 1952 (1993).

[4] Y. Berk, A. Kamenev, A. Palevski, L. N. Pfeiffer, and K. W. West, Phys. Rev. B **50**, 15 420 (1994).

[5] Y. Berk, A. Kamenev, A. Palevski, L. N. Pfeiffer, and K. W. West, Phys. Rev. B **51**, 2604 (1995).

[6] G. F. Giuliani and J. J. Quinn, Phys. Rev. B **26**, 4421 (1982).

[7] O. Entin-Wohlman and Y. Imry, Phys. Rev. B **45**, 1590 (1992).

[8] O. Entin-Wohlman and Y. Imry, Phys. Rev. B **40**, 6731 (1989).

[9] H. Gutfreund and Y. Unna, J. Phys. Chem. Solids **34**, 1523 (1973).

[10] P. T. Coleridge, Phys. Rev. B **44**, 3793 (1991).

[11] A. Schmid, Z. Phys. **271**, 251 (1974).